Electronic Supplementary Information

Cruciform Phthalocyanine Pentad-based NIR-II Photothermal Agent for Highly Efficient Tumor Ablation

Houhe Pan,[a,‡] Shukun Li,[b,‡] Jinglan Kan,[c] Lei Gong,[a] Chenxiang Lin,[a] Wenping Liu,[a] Dongdong Qi,[a] Kang Wang,[a] Xuehai Yan,[b,*] and Jianzhuang Jiang[a,*]

Caption of Content

Experimental Section

General Remarks. *N*,*N*-dimethylformamide (DMF), *N*,*N*-dimethylaminoethanol (DMAE), and *n*-pentanol were freshly distilled from Na, Na, and CaH_2 under N_2, respectively. 4,5-Bis(2,6-diisopropylphenoxy)phthalonitrile[1] and 4,5-diiodophthalonitrile[2] were synthesized according to the previous literatures.

Characterizations. MALDI-TOF mass spectra were taken on a Bruker BIFLEX III ultra-high-resolution Fourier transform ion cyclotron resonance (FT-ICR) mass spectrometer with dithranol (DIT) as the matrix. ^{1}H NMR spectra were recorded on a Bruker DPX 400 spectrometer in $CDCl_3$ (reference, δ = 7.26). Electronic absorption spectra were recorded on a Lambda 750 spectrophotometer. Elemental analysis were performed on an Elementar Vavio El III. Fluorescence spectra were recorded by a FLS-980 spectrometer, and commercially available polymethine dye IR-1048 was used as a standard for the fluorescence quantum yield (λ_{ex} = 880 nm, Φ_f= 0.004 in CH_2Cl_2).[3] The size distribution and ζ potential of NPs in aqueous solution were measured by a Malvern dynamic laser scattering (DLS) instrument (Zetasizer Nano ZS-90). Transmission electron microscope (TEM) measurement was performed on a HT7700 Hitachi TEM system with an accelerating voltage of 100 kV. Atomic force microscopy (AFM) investigation was performed on a tapping-mode atomic force microscope (Bruker MultiMode8). Irradiation was performed by a 1064 nm laser (MW-GX-1064/3000mW, China). Thermal imaging was performed using a compact thermal imaging camera (FLIR E60). Photoacoustic equipment (MSOT inVision128, iThera Medical Inc., Germany).

Synthesis of $Zn[Pc(OC_{12}H_{17})_6I_2]$ (3): A mixture of 4,5-bis(2,6-diisopropylphenoxy)phthalonitrile (2.80 g, 5.83 mmol), 4,5-diiodophthalonitrile (0.20 g, 0.53 mmol), and $ZnCl_2$ (0.50 g, 3.67 mmol) in anhydrous DMAE (8 ml) was heated at 110ºC for 8 h under N_2. After being cooled to room temperature, the solvent was evaporated. The resulting crude product was chromatographed on a silica gel column eluting with CH_2Cl_2:hexane:pyridine (v/v/v 1:4:0.01). The first green band containing $Zn[Pc(OC_{12}H_{17})_8]$ was collected, which was followed by the second green band containing $Zn[Pc(OC_{12}H_{17})_6I_2]$ (**3**). Repeated chromatography followed by recrystallization from CH_2Cl_2-CH_3OH provided $Zn[Pc(OC_{12}H_{17})_6I_2]$ (**3**) (415 mg, 41.8%). ^1H NMR (400 MHz, $CDCl_3$, 298 K): δ = 9.75 (2H, s), 8.36 (2H, s), 8.18 (2H, s), 8.14 (2H, s), 7.53 (4H, m), 7.47 (14H, m), 3.48 (12H, m), 1.34-1.26 (72H, m); MS (MALDI-TOF): Calcd. for $C_{104}H_{110}I_2N_8O_6Zn$ $[M]^+$ 1885.60; found m/z 1885.801.

Synthesis of $Zn[Pc(OC_{12}H_{17})_6(CN)_2]$ (2): A mixture of $Zn[Pc(OC_{12}H_{17})_6I_2]$ (**3**) (415 mg, 0.22 mmol), $Pd[P(Ph)_3]_4$ (25 mg, 0.022 mmol), and $Zn(CN)_2$ (52 mg, 0.44 mmol) in anhydrous DMF (3 ml) was heated at 120ºC for 3 h under nitrogen. After being cooled to room temperature, the reaction mixture was diluted with ammonium hydroxide. The precipitate was collected by filtration and washed with water, which was then chromatographed on a silica gel column using CH_2Cl_2 as eluent. Repeated chromatography followed by recrystallization from CH_2Cl_2-CH_3OH provided $Zn[Pc(OC_{12}H_{17})_6(CN)_2]$ (**2**) (358 mg, 96.6%). ^1H NMR (400 MHz, $CDCl_3$, 298 K): δ = 8.34 (2H, s), 8.24 (2H, s), 8.21 (2H, s), 7.62 (6H, m), 7.51 (12H, t), 3.48 (12H, m), 1.32-1.26 (72H, m); MS (MALDI-TOF): Calcd. for $C_{106}H_{110}N_{10}O_6Zn$ $[M]^+$ 1683.79; found m/z 1683.931.

Synthesis of Zn_4-$H_2[Pc(OC_{12}H_{17})_{24}]$ (1): A mixture of magnesium turnings (8 mg, 0.33 mmol) and a small amount of iodine in anhydrous *n*-pentanol (1.5 ml) was refluxed for 4 h (until all magnesium was consumed) under nitrogen. Then $Zn[Pc(OC_{12}H_{17})_6(CN)_2]$ (**2**) (150 mg, 0.089 mmol) was added. The resulting mixture was refluxed for another 8 h. After the mixture was cooled, the solvent was evaporated. CF_3COOH (2 ml) was added afterwards and stirred in nitrogen atmosphere for 8 h. The mixture was then poured into ice-water (20 ml) and neutralized with NH_3 H_2O. The precipitate was collected by filtration, washed several times with water, and then dried under vacuum. The residue was chromatographed on a silica gel column eluting with CH_2Cl_2. Further repeated gel-permeation chromatography using $CHCl_3$ as eluent followed by recrystallization from CH_2Cl_2 and CH_3OH gave dark green solid of Zn_4-$H_2[Pc(OC_{12}H_{17})_{24}]$ (**1**) (91 mg, 60.7%). ^1H NMR (400 MHz, $CDCl_3$, 298 K), δ = 11.53 (8H, s), 8.97 (8H, s), 8.31 (8H, s), 8.26 (8H, s), 7.65 (16H, m), 7.54 (32H, t), 7.11 (16H, d), 6.99 (8H, t), 3.72 (16H, m), 3.51 (32H, m), 2.26 (2H, s),1.37-1.28 (288H, m); UV-Vis ($CHCl_3$), λ_{max} (lgε): 291 (5.28), 363 (5.55), 653 (5.30), 824 (4.88), 901 (5.12), 1040

(5.76); MS (MALDI-TOF): Calcd. for $C_{424}H_{442}N_{40}O_{24}Zn_4$ $[M]^+$ 6744.19; found m/z 6744.011.

Synthesis of Zn_4-H_2Pc/DP NPs : To prepare Zn_4-H_2Pc/DP NPs, 1 ml of the DSPE-PEG_{2000}-OCH_3 aqueous solution (0.15 mg mL^{-1}) was rapidly injected into 50 μL DMAE/THF (v/v = 1:1) solution of Zn_4-$H_2[Pc(OC_{12}H_{17})_{24}]$ (**1**) (1 mg ml^{-1}). Repeat the above operation for 100 times and then collect all the solutions. This was followed by sonicating the mixture for 30 minutes at 500 W power (Kun Shan Ultrasonic Instruments Co., Ltd, Kunshan, PR China). For removing organic solvent, the aqueous dispersion was sealed in a dialysis bag (molecular weight cut-off: 3.5 kDa) and immersed in 5 L ultrapure water for 48 h, during which the water was replaced for 7 times. Then the solution of Zn_4-H_2Pc/DP NPs was transferred to ultra-15 ml centrifugal filters (10 kDa, Amicon Ultra-15) and centrifuged at 3900 rpm (Eppendorf Centrifuge 5810 R) for 15 min. After the centrifugation, Zn_4-H_2Pc/DP NPs retained in the upper tubes of the filters were readily diluted to different concentrations or re-dispersed by different solvents.

NMR section. Zn_4-$H_2[Pc(OC_{12}H_{17})_{24}]$ (**1**) has been characterized by ^1H NMR and ^1H-^1H COSY spectroscopy, all the signals could be assigned to respective proton species in an unambiguous manner. As shown in Fig. S4, the ^1H NMR spectrum of **1** exhibits four singlets at δ = 11.53 (2 H), 8.97 (2 H), 8.31 (2 H), and 8.26 (2 H) ppm for the *á* protons. The one multiplet at δ = 7.65 (16 H) ppm, one triplet at δ = 7.54 (32 H) ppm, one doublet at $\delta = 7.11$ (16 H) ppm, and one triplet at $\delta = 6.99$ (8 H) ppm can be assigned to three types of the aromatic protons of the â-substituted 2,6-diisopropylphenoxy groups with the help of their ^{1}H-^{1}H COSY spectra. The isopropyl protons are observed at δ 3.72 (16 H), 3.52 (32 H), and 1.37-1.28 (288 H) ppm. Different from mononuclear Pcs, one signal at 2.26 (2 H) ppm, other than negative field, is attributed to the pyrrole protons in the central Pc ring, which is affected by not only the circular current shielding effect of central Pc ring, but also circular current deshielding effect of the peripheral Pc rings.

Measurement of Photothermal Performance

Aqueous solutions of Zn_4-H_2Pc/DP NPs (1.0 ml) with different concentrations (0 ppm to 54 ppm of **1**) were led to a quartz cuvette, then were irradiated with a 1064 nm light at a series of power density between 0.3-1.5 W cm^{-2} for 15 min at room temperature (~25°C). Ultrapure water was used as a control group. A thermocouple probe with a digital thermometer was used to measure the temperature every 10 s with an accuracy of 0.1°C.

Photothermal conversion efficiency was evaluated by recording the change in the temperature of the aqueous solution of Zn_4-H_2Pc/DP NPs (1.0 ml, 27 ppm of **1**) as a function of time under continuous irradiation of 1064 nm laser with a power density of 0.9 W cm^{-2} until the solution reached a steady-state temperature. Photothermal conversion efficiency, η, was calculated using Eq. (1):

$$\eta = \frac{hS(T_{max} - T_{surr}) - Q_{Dis}}{I(1 - 10^{-A_{1064}})} \tag{1}$$

where h is the heat transfer coefficient, S is the surface area of the container, T_{Surr} and T_{max} are initial (24.7°C) and final equilibrium temperature (50.5°C) of the solution. Q_{Dis} represents the heat dissipation from the light absorbed by the quartz sample cell (0.0257 W), I is incident laser power (0.704 W), and A_{1064} is the absorbance of Zn_4-H_2Pc NPs at 1064 nm (1.419). The value of hS is derived according to Eq. (2):

$$\mathbf{hS} = \frac{\sum m_i C_i}{\tau_S} \tag{2}$$

where m and C are the mass (1.0 g) and heat capacity (4.2 J g^{-1}) of the deionized water used as solvent, respectively. τ_S is the sample system time constant calculated by the following Eq. (3):

$$\tau_S = \frac{t}{ln\theta} \tag{3}$$

where θ is the dimensionless driving force and t is time.

Tissue-penetration photothermal ability

100 μl of Zn_4H_2Pc/DP NPs dispersion (81 ppm) was filled in a 96-well plate, which covered by chicken breast muscles of various thickness (0, 1, and 4 mm) on top. This was then irradiated under 1064 nm light (1.0 W cm^{-2}) for 6 min. In the meantime, the IR thermographs were captured every 20 seconds by a thermal imaging camera (FLIR E60).

Computational details

Density functional theory (DFT) and time-dependent DFT (TD-DFT) calculations were carried out at the level of M06L/6-31G(d) level.[4] Vibrational analysis is also employed to confirm the optimized structure. All the calculations are carried out using Gaussian 09 D.01 Program.[5]

Cell culture and PTT *in vitro*

MCF-7 cells were purchased from Shanghai Institute of Biochemistry. Cell Biology were cultured in DMEM containing 10% FBS at 37 °C in humidified ambiance of 5% CO_2. Cells were seeded in 96-well plates at a density of 2.5×10^4 cells per well and were incubated for 24 h for *in vitro* PTT. Then, Zn_4-H_2Pc/DP NPs were diluted to different concentrations in wells, incubated with the cells for 24 h. After being washed with fresh culture medium, the cells were exposed to 1064 nm laser at 1.5 W cm^{-2} for 1 min. And then, the cells were incubated in dark for another 24 h before the cell viability was investigated by the MTT method.

Animals and tumor model

All animal investigations conformed to the protocols approved by the local Ethical Committee on the basis of the Chinese law. BALB/c-nude mice (female) were obtained from Beijing HFK Bioscience Co. Ltd. MCF-7 cells (6×10^7 cells ml^{-1}, 100 μl) were injected the sub-dermal dorsal area of each mouse. The tumor dimensions were monitored with a vernier caliper. The tumor volume was calculated by length × $width^2$ / 2.

PA imaging *in vitro* and *in vivo*

For *in vitro* PA imaging, various concentrations (0, 9, 18, 37, 75, 150, 300 ppm) of Zn_4-H_2Pc/DP NPs in aqueous solution were led to a cylindrical vessel prepared by agarose gel and scanned from 700 to 960 nm using a MSOT equipment. For *in vivo* PA imaging, tumor-bearing mice were injected intratumorally with 50 μl Zn_4-H_2Pc/DP NPs (600 ppm in aqueous 5% glucose solution) and monitored in 900 nm by MSOT equipment at various time points.

PTT *in vivo*

The mice were treated with PTT, after the tumor volumes reached about 100 mm^3. Ten mice were randomized into two groups: Control group (laser only) and NPs group (Zn_4-H_2Pc/DP NPs + laser). For NPs group, mice were intratumorally injected with 50 μl Zn_4-H_2Pc/DP NPs (600 ppm) in aqueous 5% glucose solution. After 4 h post-injection, all the mice were fixed by medical adhesive tape, and then their tumor regions were irradiated by a 1064 nm light (0.6 W cm^{-2}) for 10 min. During irradiation IR images of mice were monitored by a compact thermal imaging camera (FLIR E60). After PTT, the tumor sizes and body weights were recorded every day.

Statistical analysis

All experiments were repeated at least three times. Data are expressed as mean ± standard deviation. Statistical significance was determined using one-way analysis of variance (ANOVA), with P < 0.05 considered to be statistically significant.

References

[1] Pan H, Liu W, Wang C, et al. Chemistry-A European Journal, 2016, 22(28): 9488-9492.

[2] Dokládalová L, Bureš F, Kuznik W, et al. Organic & biomolecular chemistry, 2014, 12(29): 5517-5527.

[3] Furuyama T, Satoh K, Kushiya T, et al. Journal of the American Chemical Society, 2013, 136(2): 765-776.

[4] Zhao Y, Truhlar D G. The Journal of chemical physics, 2006, 125(19): 194101.

[5] Frisch M. J., et al. Gaussian 09, Revision D.01, Gaussian, Inc., Wallingford, Connecticut, U.S.A., 2009.

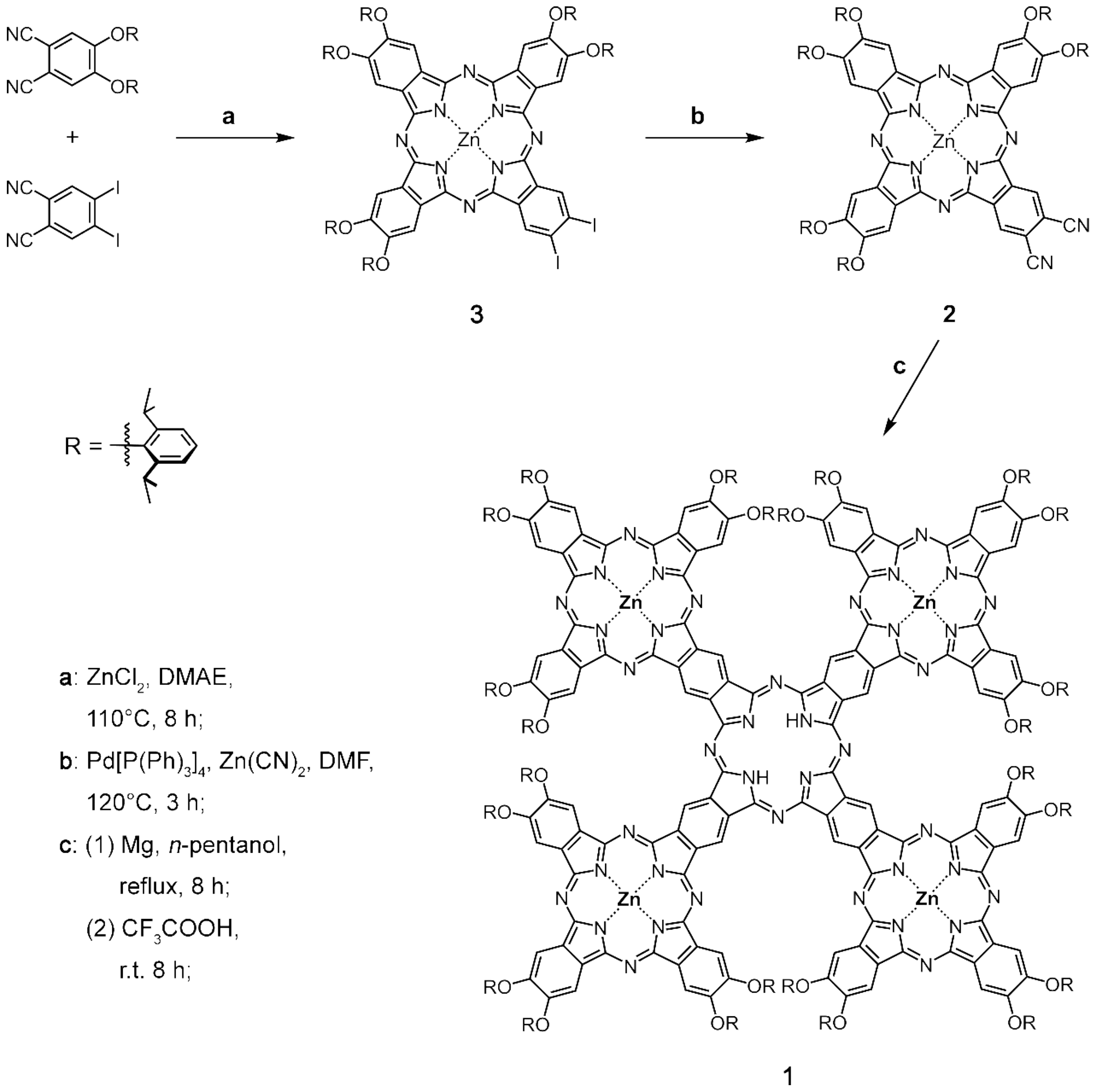

Scheme S1. Synthesis of cruciform phthalocyanine pentad.

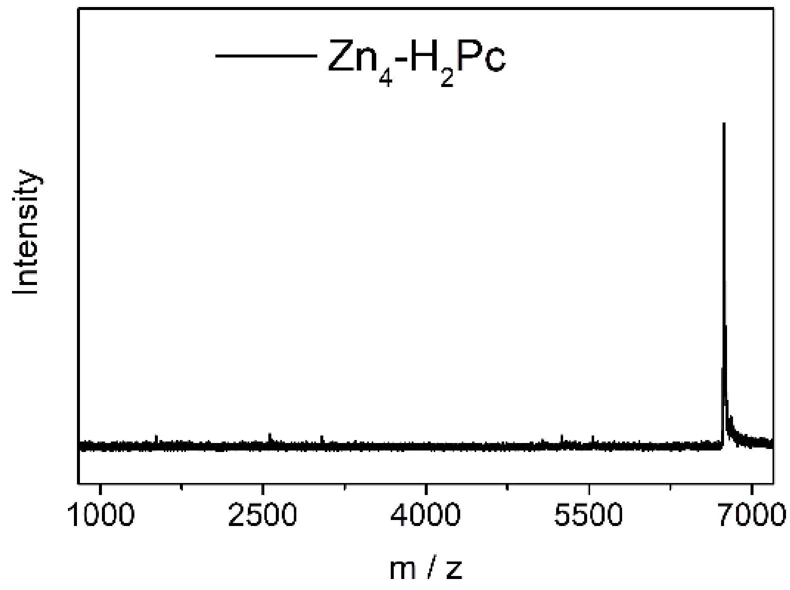

Fig. S1. The molecular ion of Zn_4-$H_2[Pc(OC_{12}H_{17})_{24}]$ (**1**) shown in the MALDI-TOF mass spectra.

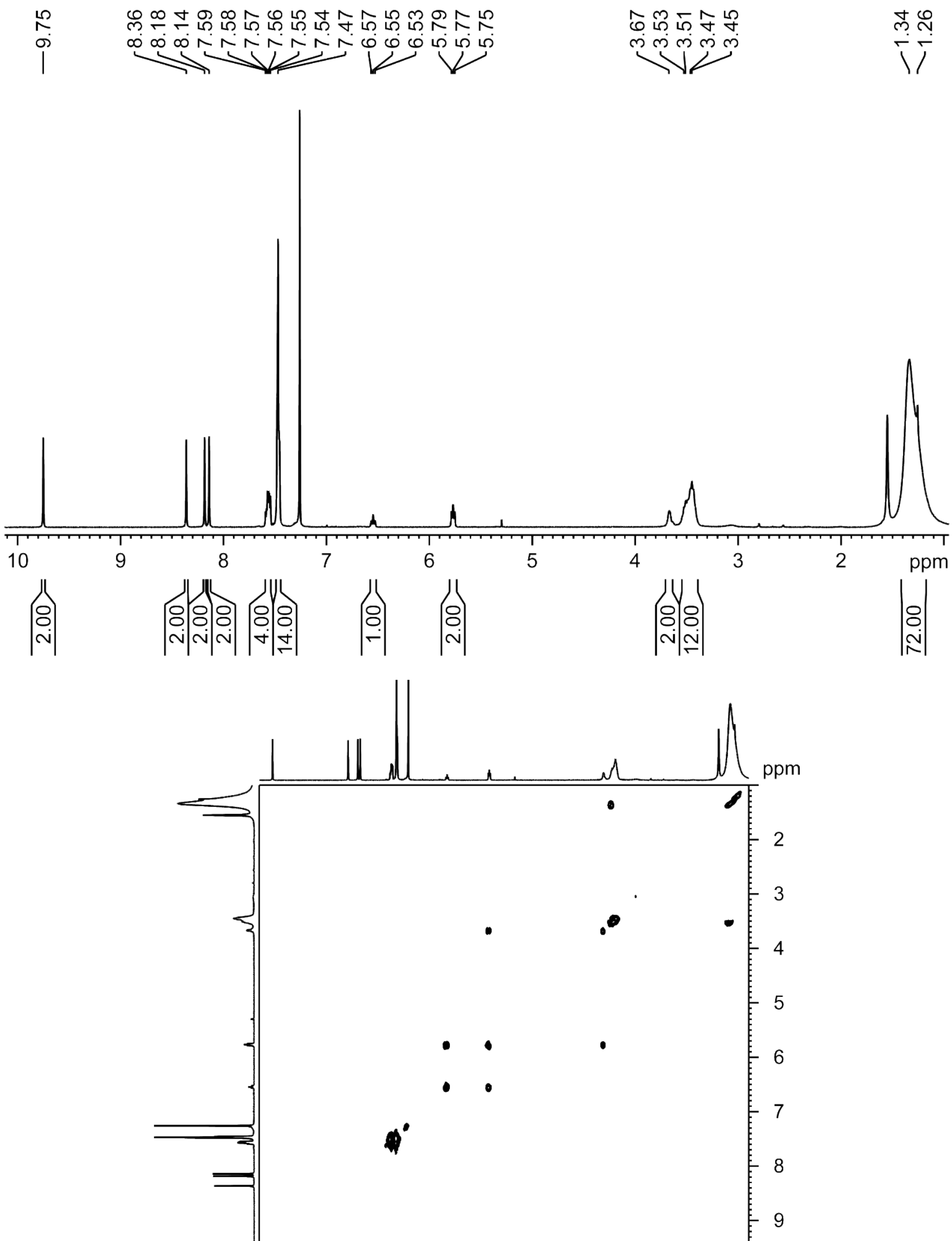

Fig. S2. ^{1}H NMR and ^{1}H-^{1}H COSY spectra for $Zn[Pc(OC_{12}H_{17})_6I_2]\cdot C_5H_5N$ recorded in $CDCl_3$.

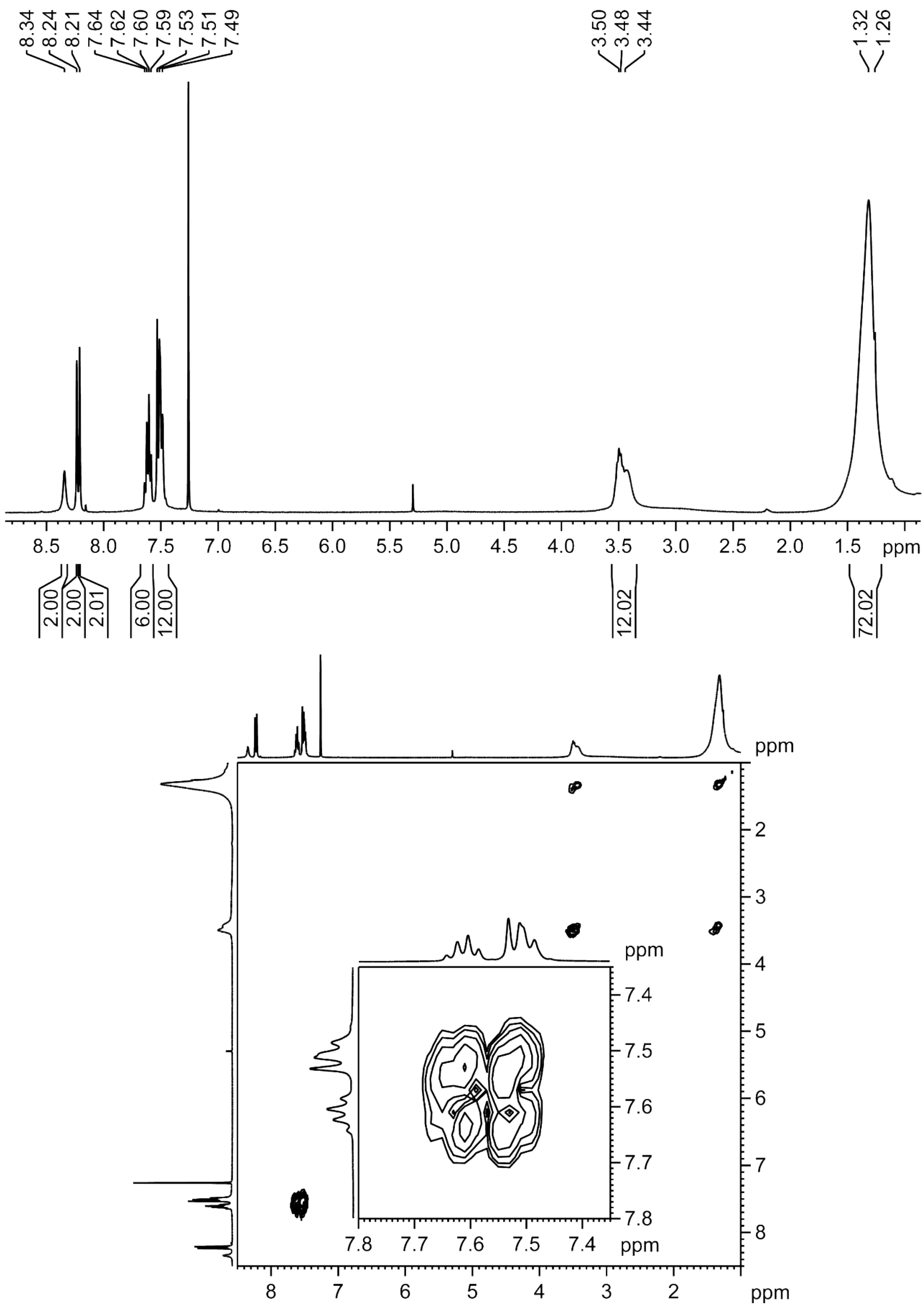

Fig. S3. ^{1}H NMR and ^{1}H-^{1}H COSY spectra for $Zn[Pc(OC_{12}H_{17})_6(CN)_2]$ (**2**) recorded in $CDCl_3$.

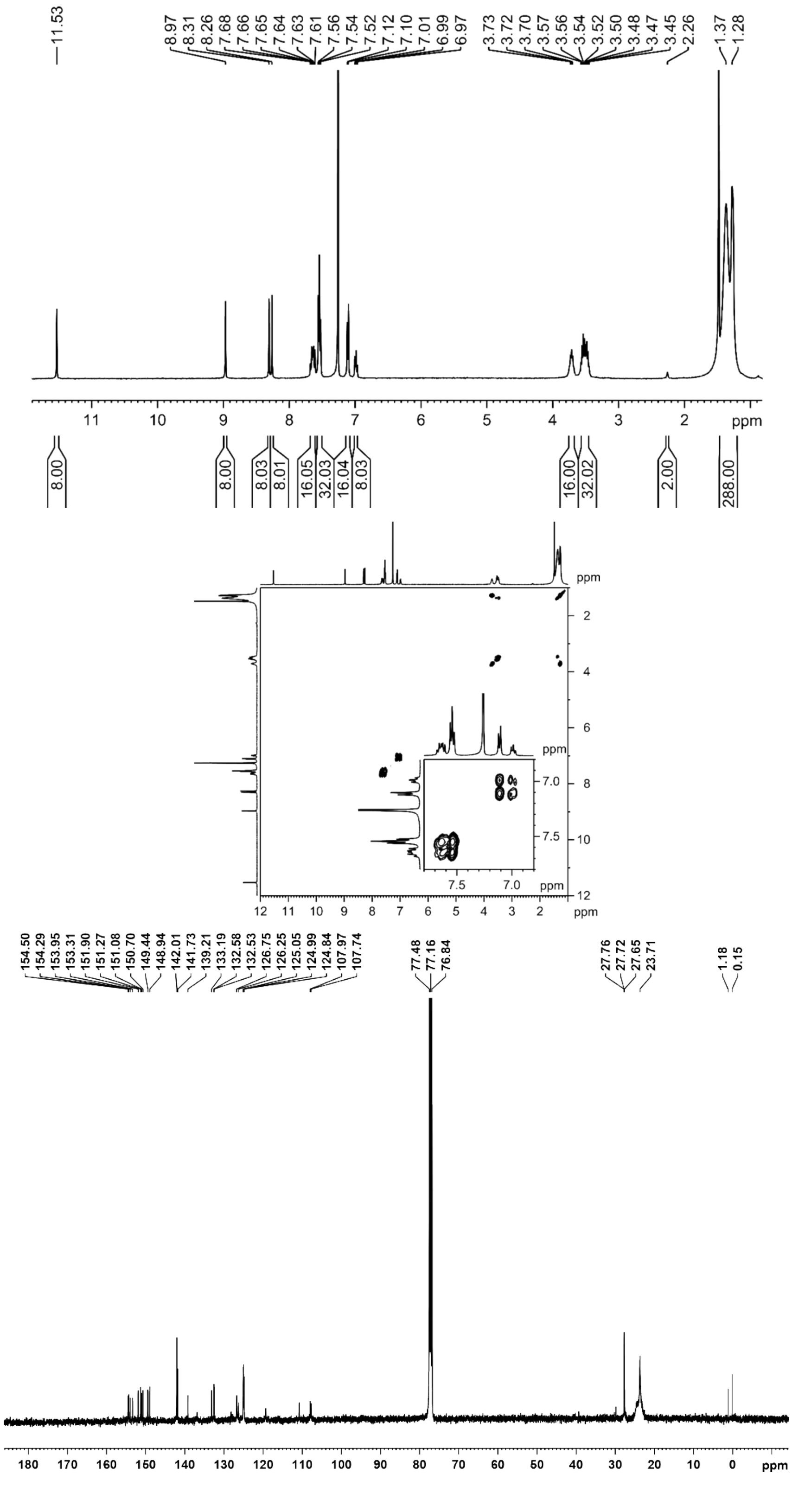

Fig. S4. ^{1}H NMR, ^{1}H-^{1}H COSY and ^{13}C NMR spectra for Zn_4-$H_2[Pc(OC_{12}H_{17})_{24}]$ (**1**) recorded in $CDCl_3$.

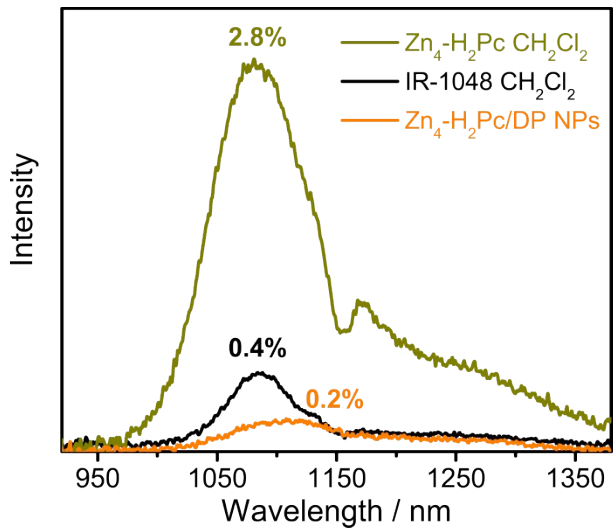

Fig. S5. The fluorescence emission spectra of Zn_4-$H_2[Pc(OC_{12}H_{17})_{24}]$ (**1**) and IR-1048 in CH_2Cl_2 and Zn_4-H_2Pc/DP NPs in water (λ_{ex} = 880 nm).

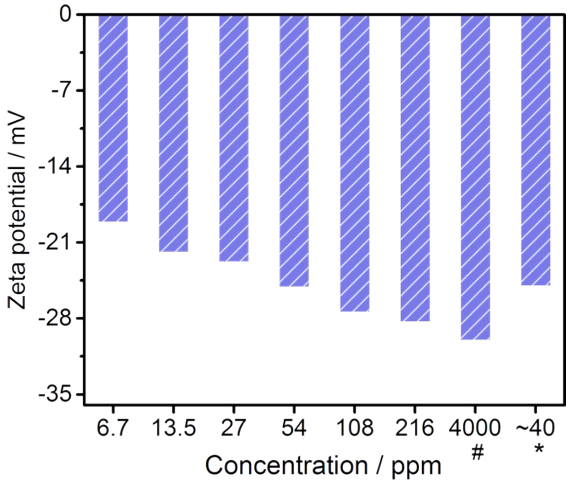

Fig. S6. The ζ potentials for various concentrations of Zn_4-H_2Pc/DP NPs in aqueous solution

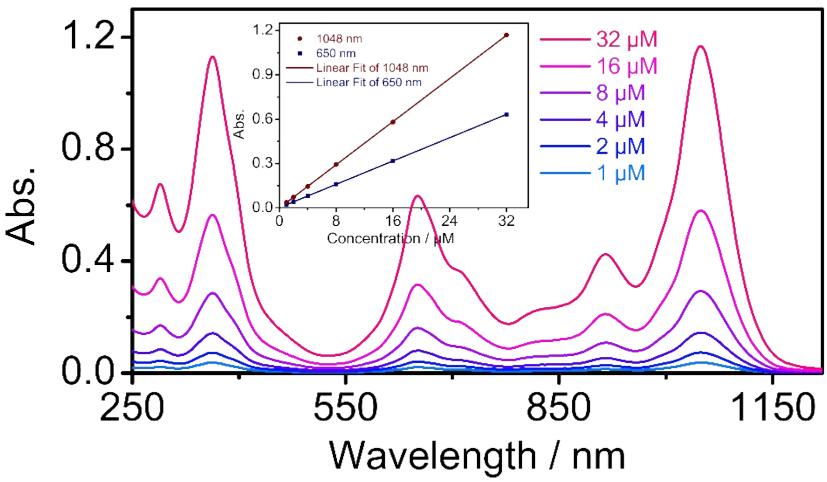

Fig. S7. Electronic absorption spectra of Zn_4-H_2Pc/DP NPs in aqueous solution at concentrations ranging from 1 to 32 μM. The insert shows a plot of absorbance versus concentration (cuvette path-length: 1 mm).

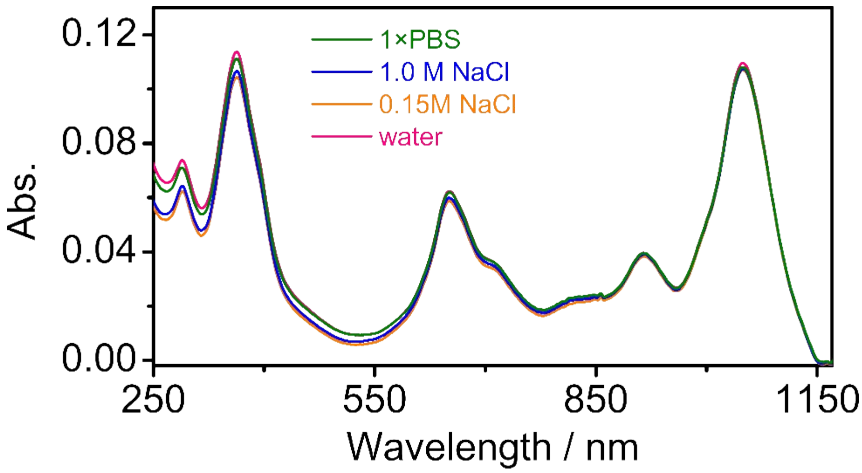

Fig. S8. Electronic absorption spectra of Zn_4-H_2Pc/DP NPs in various aqueous solution (cuvette path-length: 1 mm).

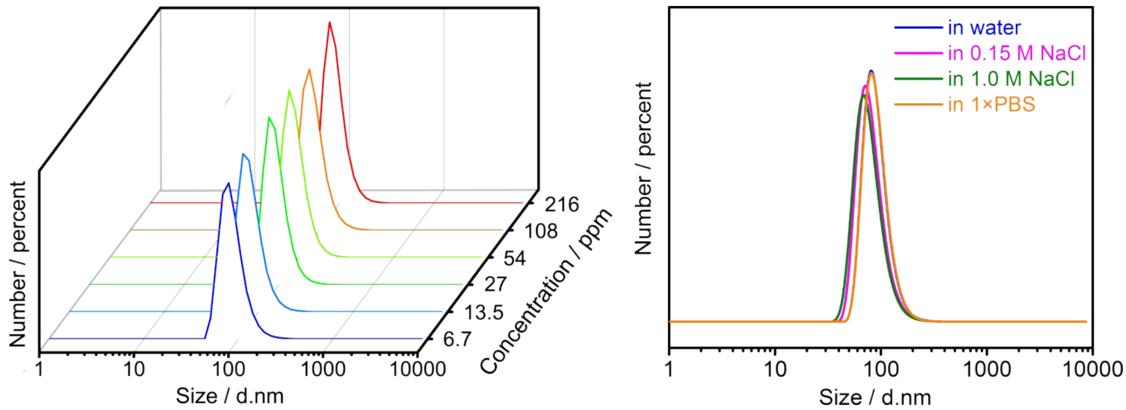

Fig. S9. The size distribution for various concentrations of Zn_4-H_2Pc/DP NPs in different aqueous solution.

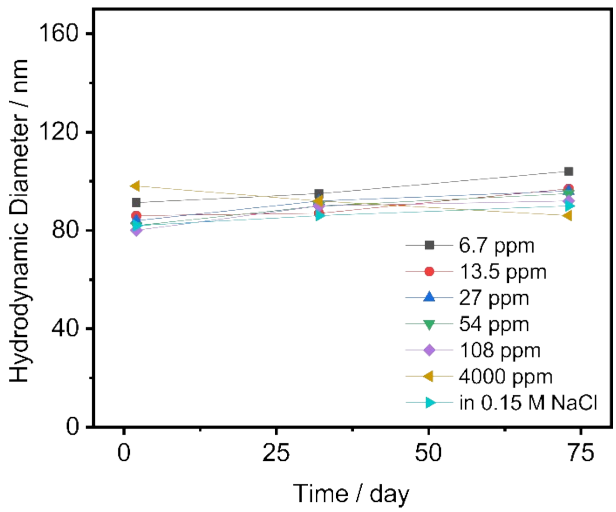

Fig. S10. The DLS stability of Zn_4-H_2Pc/DP NPs in various solutions for 73 days.

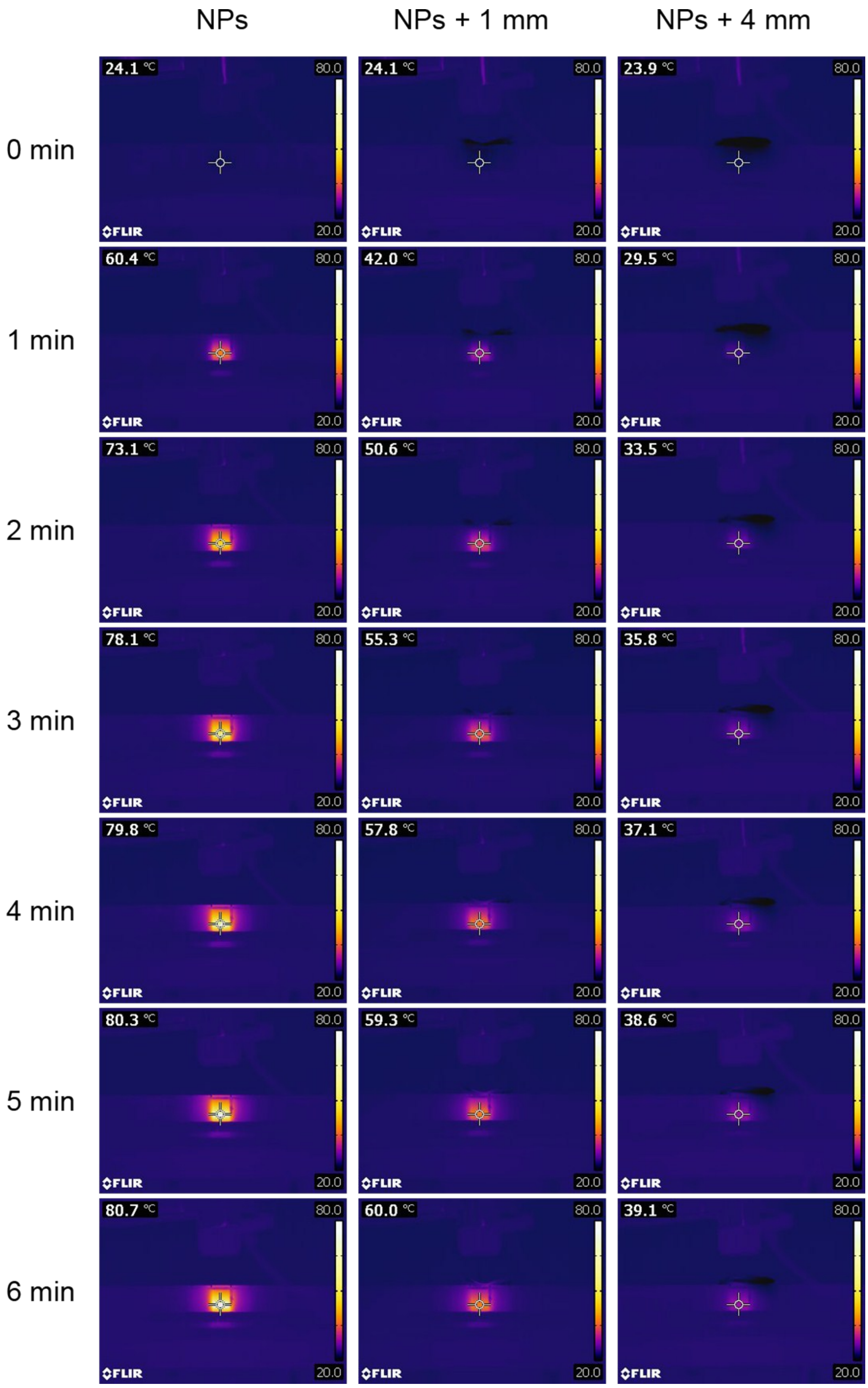

Fig. S11. Representative thermal images of 100 µl Zn_4-H_2Pc/DP NPs solution (81 ppm) under 0, 1, and 4 mm thick tissue at different time points.

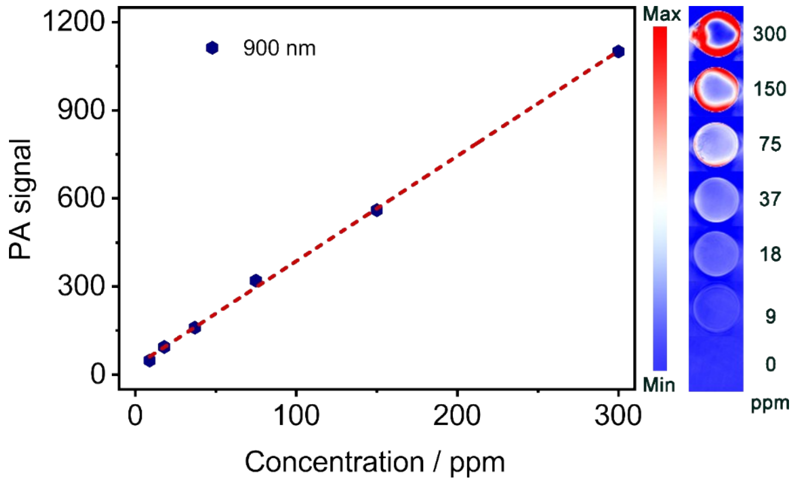

Fig. S12. The PA signal intensity as a function of concentrations of Zn_4-H_2Pc/DP NPs. Right: PA images of Zn_4-H_2Pc/DP NPs at various concentrations.

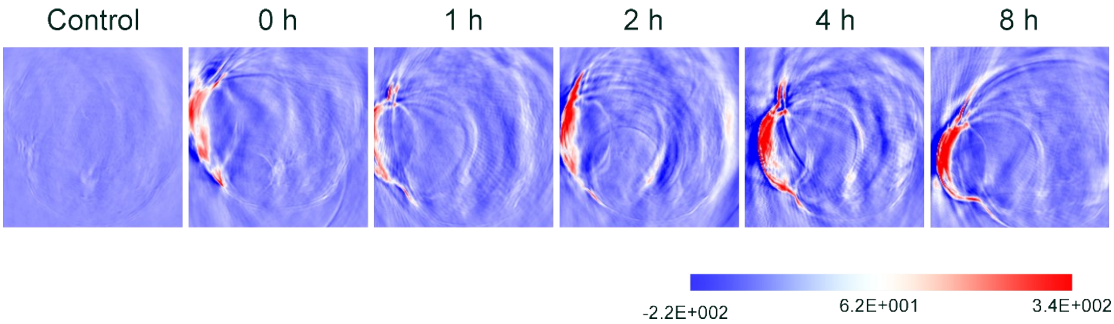

Fig. S13. PA imaging in the tumor site of tumor-bearing mice intratumorally injected with 50 µl Zn_4-H_2Pc/DP NPs solution (600 ppm).

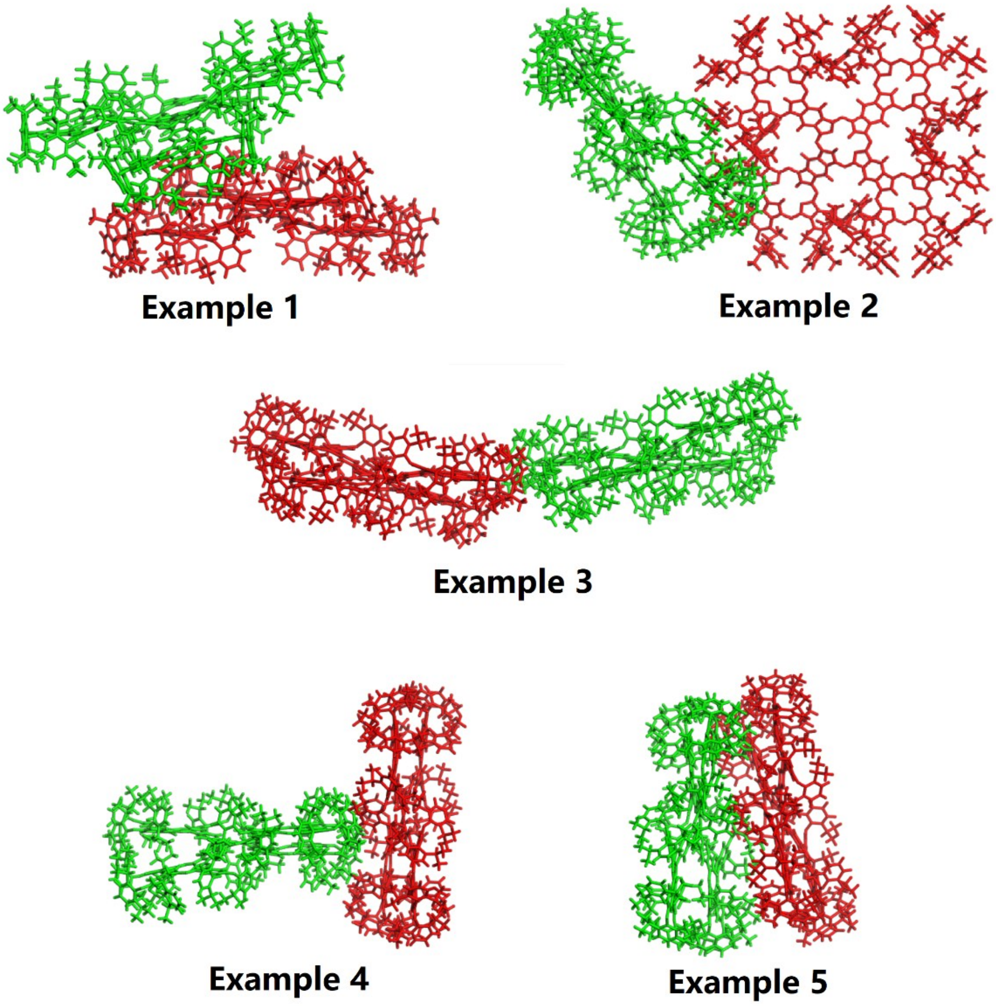

Fig. S14. A few examples of the various molecular 1 assembling forms in the nanoball. Due to the existance of huge periferal -Ph[CH(CH_3)$_2$]$_2$ substituents, the Pc macrocycle is rarely able to get close to each other, The binding force between two molecules comes from the Van der Waals attractions of {Ph[CH(CH_3)$_2$]$_2$ ~ Ph[CH(CH_3)$_2$]$_2$} and { Ph[CH(CH_3)$_2$]$_2$ ~ Pc }.

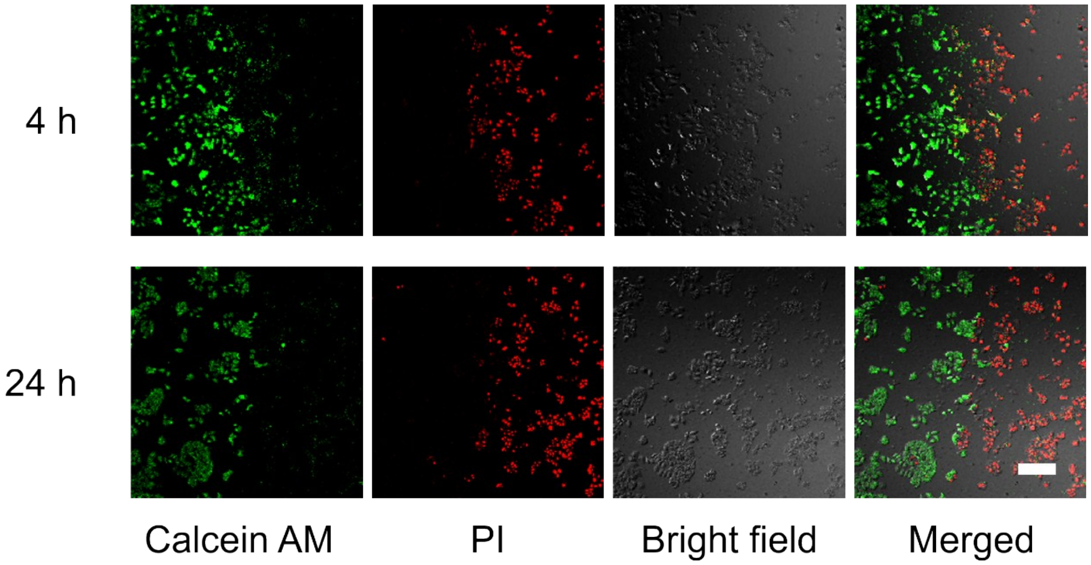

Fig. S15. CLSM images of calcein AM and PI costained MCF-7 cells incubated with 250 ppm Zn_4-H_2Pc/DP NPs for 4 and 24 h, under 1064 nm laser irradiation (1.2 W cm^{-2}, 3 min). Images share the same scale bar (200 μm).

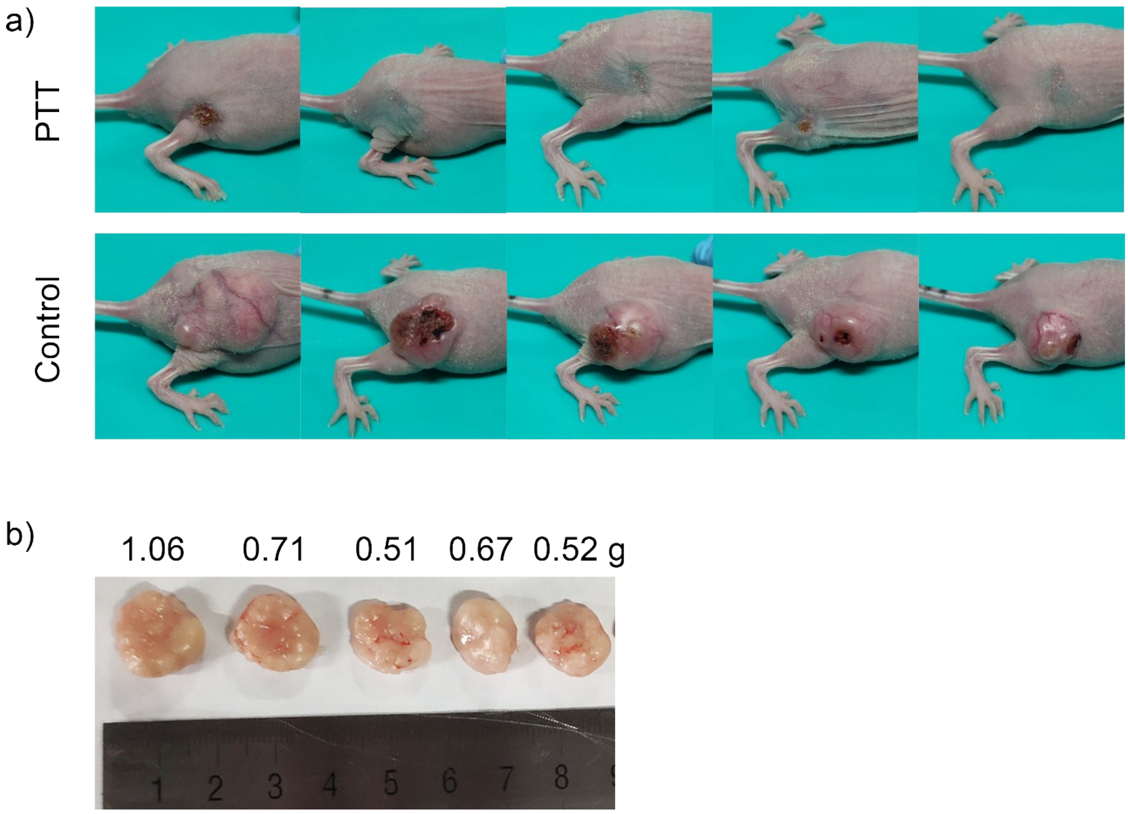

Fig. S16. Photos of all a) the mice or b) tumors at the end of the observation (20 day).

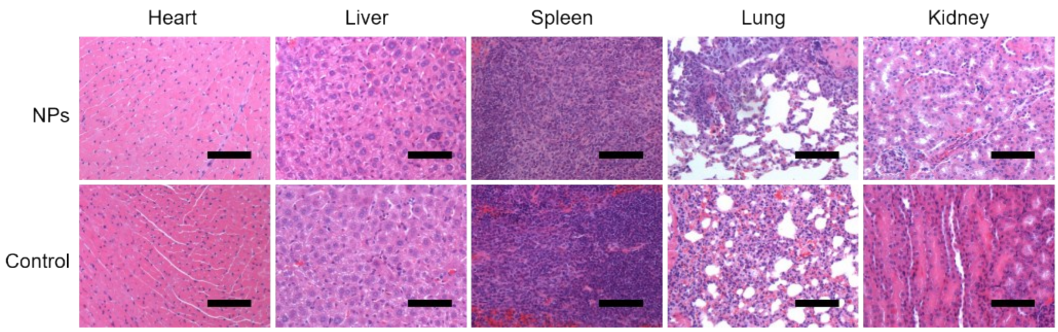

Fig. S17. Representative H&E stained images of major organs (heart, liver, spleen, lung, and kidneys) from the Control and NPs Group mice at 21 days post-treatment. Scale bar: 100 μm.

Table S1. Elemental analytical and mass spectrometric data for Zn_4-$H_2[Pc(OC_{12}H_{17})_{24}]$ (**1**).[a]

Compound	Chemical Formula	$M^+(m/z)$[b]	Analysis		
			C	H	N
1	$C_{424}H_{442}N_{40}O_{24}Zn_4$	6733.190987 (6733.176693)	75.45 (75.51)	6.54 (6.61)	8.39 (8.31)

[a] Calculated values given in parentheses. [b] By MALDI-TOF mass spectrometry.

Table S2. ^{1}H NMR spectra for **1-3** in $CDCl_3$.

compound	Pc-Hα	OPh-H	Other H	-C**H**$(CH_3)_2$	-CH(C**H**$_3)_2$
$Zn[Pc(OC_{12}H_{17})_6I_2]$ (**3**)	9.75 (2H, s) 8.36 (2H, s) 8.18 (2H, s) 8.14 (2H, s)	7.53 (4H, m) 7.47 (14H, m)	Axial-pyridine 6.55 (1H, t) 5.77 (2H, t) 3.67 (2H, s)	3.48 (12H, m)	1.34-1.26 (72H, m)
$Zn[Pc(OC_{12}H_{17})_6(CN)_2]$ (**2**)	8.34 (2H, s) 8.24 (2H, s) 8.21 (2H, s)	7.62 (6H, m) 7.51 (12H, t)		3.48 (12H, m)	1.32-1.26 (72H, m)
Zn_4-$H_2[Pc(OC_{12}H_{17})_{24}]$ (**1**)	11.53 (8H, s) 8.97 (8H, s) 8.31 (8H, s) 8.26 (8H, s)	7.65 (16H, m) 7.54 (32H, t) 7.11 (16H, d) 6.99 (8H, t)	N-H 2.26 (2H, s)	3.72 (16H, m) 3.51 (32H, m)	1.37-1.28 (288H, m)

Table S3. Electronic absorption data of Zn_4-H_2[Pc($OC_{12}H_{17}$)$_{24}$] (**1**) in $CHCl_3$ and Zn_4-H_2Pc/DP NPs in water.

compound	λ_{max}/nm (lgε)					
1	291 (5.28)	363 (5.55)	653 (5.30)	824 (4.88)	901 (5.12)	1040 (5.76)
NPs	290 (5.32)	362 (5.55)	650 (5.30)	--	916 (5.12)	1048 (5.56)